Refractive-Index Matching Avoids Local Field Corrections and Scattering Bias in Solid-State Na_2SO_4 Ultraviolet Raman Cross-Section Measurements

LULING WANG and SANFORD A. ASHER*

Department of Chemistry, University of Pittsburgh, Pittsburgh, Pennsylvania 15260

We report a refractive-index matching method to measure nonabsorbing solid ultraviolet (UV) Raman cross-sections that avoids the local field correction and interface scattering of incident light. We used refractive-index-matched chloroform as an internal standard to determine the solid-state 995 cm^{-1} Na_2SO_4 244 nm Raman cross-sections. The pure liquid chloroform 668 cm^{-1} 244 nm Raman cross-section was determined by using acetonitrile as an internal standard and by calculating the local field corrections for the observed Raman intensities. Our measured 244 nm UV Raman cross-section of the solid-state 995 cm^{-1} SO_4^{2-} band of 1.97 ± 0.07 × 10^{-28} $cm^2/(molc \cdot sr)$ is about half of its aqueous solution Raman cross-section, indicating interactions between the sulfate species in the solid that decrease the Raman polarizability.

Index Headings: **Solid Raman cross-section; Refractive-index matching; Local field corrections; UV Raman spectroscopy.**

INTRODUCTION

Raman spectroscopy is a powerful method for studying molecular structure and environment.[1–3] The Raman intensities observed are proportional to the molecular Raman cross-sections. Thus, Raman intensities can be used to determine molecular concentrations if the Raman cross-sections are known, if and only if the excitation beam sampling is defined with respect to the collection optics.[4] Unfortunately, direct measurements of Raman cross-sections are very difficult because the measurements require a detailed understanding of both the incident laser light excitation geometry (including the excitation beam attenuation within the sample), the effective Raman scattered light collection solid angle, as well as the transfer efficiency of the spectrometer.[5–9]

Most previous studies of Raman cross-sections measured the Raman cross-sections of liquid solutions by using internal standards with known Raman cross-sections.[10–18] Some of these studies[10,18] directly reference their relative intensity measurements to the determination of the absolute Raman cross-section of benzene at 514.5 nm by Kato et al.[5] and Abe et al.,[19] while others[11–17] reference their measured intensities to more recently measured Raman cross-sections that, however, were also referenced to benzene. The internal standard methods are relatively easy and quite accurate for measuring Raman cross-sections for liquids or species in solution.

In contrast, there are very few measurements of Raman cross-sections of solids.[20–22] Raman cross-section measurements of solids are more challenging because it is more difficult to homogeneously disperse different species in order to use internal standard methods. Many analytically important applications require determination of the concentrations of solid-state materials. This is the case for explosive materials, for example, which are almost always found in the solid state.[20]

We recently developed a method to disperse sub 20 nm solid particles in the interstices of close-packed silica photonic crystals.[23] This created a solid-state sample in which the individual particles were too small to attenuate the resonant incident exciting light or the Raman scattered light traversing individual particles. This prevented self-absorption bias in the measurement such that the relative intensities observed were proportional to the solid-state particle Raman cross-sections.

We achieved intimate mixing of the <20 nm particles of the analyte and the internal standard by sublimating a frozen solution containing both the analyte and internal standard species that filled the nanosize interstices of a close-packed silica opal photonic crystal. In order to determine the solid Raman cross-section of the analyte solid particles we needed to determine the Raman cross-sections of a convenient solid-particle internal standard.[23]

In the work here we demonstrate a refractive-index matching method used to determine the Raman cross-sections for solid nonabsorbing Na_2SO_4 particles. We use pure chloroform as an internal standard because it has a 244 nm refractive index of ~1.53,[24] almost identical to that of solid Na_2SO_4.[25] In addition, it does not dissolve Na_2SO_4. Refractive index matching the solid Na_2SO_4 particles avoids any scattering by the particle–solvent interface, which would limit the particle penetration of the excitation wavelength. We determined the 244 nm UV Raman cross-section of chloroform by measuring the Raman intensity ratio of chloroform to that of acetonitrile in a chloroform : acetonitrile solution. We determined the Raman cross-section of chloroform in the neat solvent by calculating the local field correction. We then suspended the rapidly mixed, finely ground solid Na_2SO_4 particles in neat chloroform in order to measure the 244 nm UV Raman intensity ratio of the solid Na_2SO_4 particles relative to chloroform.

EXPERIMENTAL

UV Raman Spectroscopy Instrumentation. The spectroscopic instrumentation has been described in detail elsewhere.[26,27] Raman spectra were excited with the 244 nm line of a continuous wave (CW) UV Argon Laser (Innova 300 FReD, Coherent Inc.). The samples were stirred rapidly in a sealed fused-silica cylindrical quartz cell with a 10 mm light path. The laser excitation excited the sample in a backscattering geometry with a beam spot size of ~25 μm. The Raman scattered light was dispersed and detected by a Spex Triplemate Spectrograph and a Princeton Instruments charge-coupled device (CCD)

Received 7 September 2011; accepted 31 October 2011.
* Author to whom correspondence should be sent. E-mail: asher@pitt.edu.
DOI: 10.1366/11-06468

0003-7028/12/6602-0157$2.00/0

camera (Spec-10 System, Model 735-0001). Neat acetonitrile was used for the Raman shift calibration.

UV Raman Measurements of Acetonitrile, Chloroform, and Chloroform/Acetonitrile. The chloroform/acetonitrile mixture was prepared by mixing a volume ratio of 1 : 3 of the two liquids. We consecutively collected three spectra of 1.5 s accumulations each. No UV Raman spectral differences were evident between consecutive spectra. This indicates a lack of sample degradation, even though the $CHCl_3$ absorbs some of the laser light (molar absorptivity of 0.0743 $L{\cdot}mol^{-1}{\cdot}cm^{-1}$, calculated from the pure chloroform UV-Vis absorption spectrum (Fig. 1)).

UV Raman Measurements of Chloroform and Na_2SO_4/Chloroform Dispersion. Anhydrous solid Na_2SO_4 was finely ground using a mortar and pestle. Figure 2 shows a micrograph of ground solid Na_2SO_4 particles showing an average diameter of <30 μm. The finely powdered Na_2SO_4 was suspended in neat chloroform at Na_2SO_4 concentrations of 23.6 mg/mL (mole ratio 1 : 73.7), 29.8 mg/mL (mole ratio 1 : 58.1), and 86.6 mg/mL (mole ratio 1 : 19.6). The sample was rapidly stirred to produce a homogeneous suspension in the cylindrical fused quartz sample cell. For each sample, Raman spectra were obtained at, at least, three different heights; the similarity of the spectra indicated sample homogeneity. Each measurement was repeated at least three times with 15 s accumulations each. The Raman spectra were similar, indicating that no sample degradation occurred.

UV Raman Measurements of Acetonitrile and Na_2SO_4/Acetonitrile. For comparison, we also measured UV Raman spectra of finely powdered Na_2SO_4 suspended in non-refractive-index-matched acetonitrile at Na_2SO_4 concentrations of 19.4 mg/mL (mole ratio 1 : 136.6), 29.0 mg/mL (mole ratio 1 : 90.6), and 52.1 mg/mL (mole ratio 1 : 48.8) using a method identical to that for solid Na_2SO_4 particles in chloroform, as described above.

RESULTS AND DISCUSSION

Dependence of Raman Cross-sections on the Local Field. Equation 1 shows the expression for the Raman cross-section $\sigma(\nu_0)$, where ν_0 and ν are the frequencies (cm^{-1}) of the excitation light and the molecular vibrational frequency, b is the zero-point amplitude of the vibrational mode, g is the vibrational mode degeneracy, α' is the symmetric and γ' is the anisotropic invariant of the polarizability tensor, ρ_s is the depolarization ratio for linearly polarized incident light, **e** and **e**′ are the electric field polarization vectors of the exciting light and the Stokes scattered light, and L is a local field correction factor associated with the increase in the Raman intensity of the analyte in the condensed phase of refractive index n compared to that of the isolated molecule in the gas phase.[28,29] L is described by Eq. 2, where n_0 and n_s are the *homogeneous* sample refractive indices at ν_0 and $\nu_0 - \nu$. [28,29]

$$\sigma(\nu_0) = \frac{(2\pi)^4}{45} b^2 g \frac{(\nu_0 - \nu)^4}{1 - \exp\left(-\frac{hc\nu}{kT}\right)} \cdot (45\alpha'^2 + 7\gamma'^2)\left[\frac{\rho_s + (1-\rho_s)\cdot|\mathbf{e}\cdot\mathbf{e}'|^2}{1+\rho_s}\right]\cdot L \quad (1)$$

$$L = (n_s/n_0)(n_s^2+2)^2(n_0^2+2)^2/81 \quad (2)$$

Many previous studies have demonstrated that the ratio of Raman cross-sections of a molecule dissolved within its own pure liquid state (σ_ℓ) to that as a solute molecule (σ_m) in solution is proportional to the ratio of the local field correction factors of the pure liquid (L_ℓ) to that of the solution (L_m) as described by Eq. 3, where the refractive indices n_ℓ and n_m are those of the pure liquid and of the solution samples of the molecule, respectively:[19,30,31]

$$\frac{\sigma_m}{\sigma_\ell} = \frac{L_m}{L_\ell} = \left[\frac{3}{(n_\ell/n_m)^2+2}\right]^4 \quad (3)$$

This local field correction accounts for the increase in the electromagnetic field associated with the polarization of the environment around the Raman scattering molecule. The observed Raman intensity (I) is described by Eq. 4, where N is the number of molecules contained in the illuminated volume whose Raman scattering is transferred into the spectrometer. I_0 is the intensity of the excitation beam. $F(n, \theta)$ is the fraction of the scattered light imaged into the spectrometer, which depends upon the solid angle collected (θ), which depends upon the

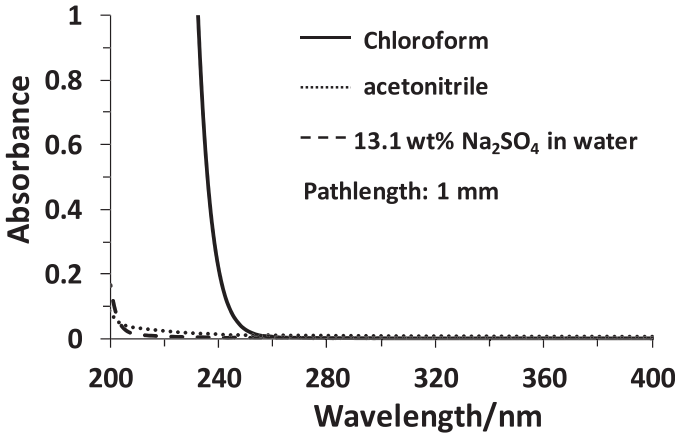

FIG. 1. UV-Vis absorbance spectra of pure chloroform, pure acetonitrile, and 13.1 wt% Na_2SO_4 in water.

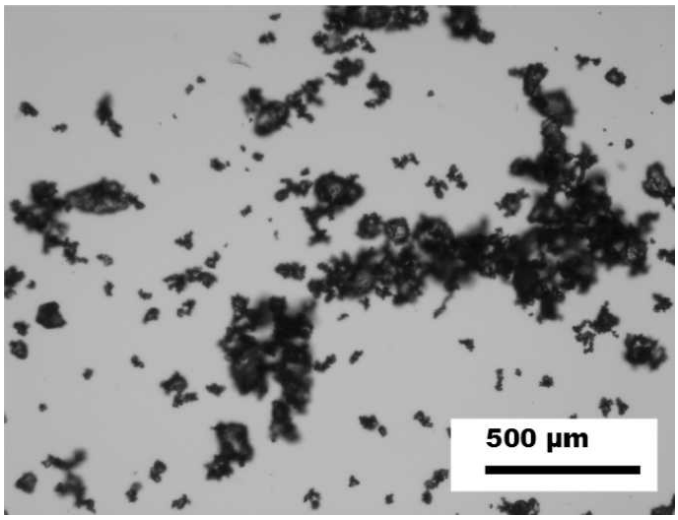

FIG. 2. Optical image of ground solid Na_2SO_4 particles.

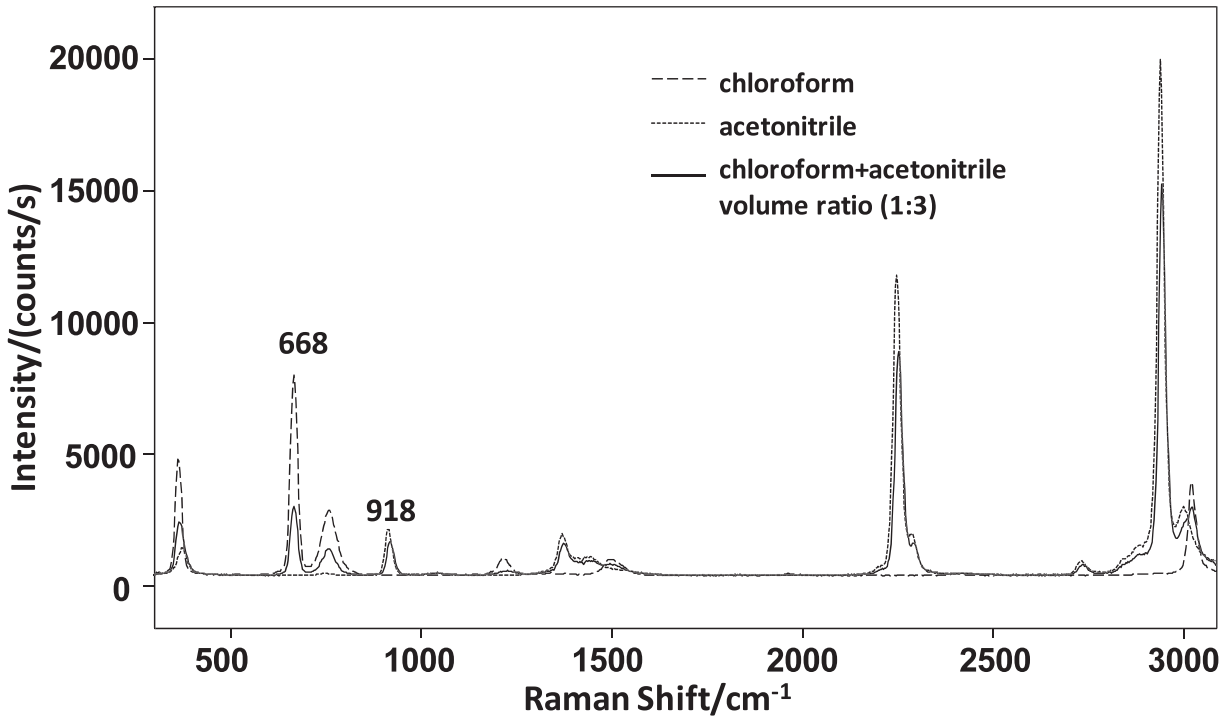

FIG. 3. UV Raman spectra of chloroform (dashed line), acetonitrile (dotted line), and chloroform/acetonitrile mixture (volume ratio, 1 : 3, solid line).

sample refractive index (n) at the Raman scattered frequency. $S(\nu_0 - \upsilon)$ is a complex factor describing the efficiency of light collection from the sample volume elements whose scattering is transferred into the spectrometer. It recognizes attenuation of the excitation beam and Raman scattered light within the sample by phenomena such as absorption and sample scattering. $E(\nu_0 - \upsilon)$ is the throughput efficiency of the spectrometer at the Raman scattered frequency.[10]

$$I(\nu_0) = NI_0F(n,\theta)S(\nu_0 - \upsilon)E(\nu_0 - \upsilon)\sigma(\nu_0) \tag{4}$$

The observed Raman intensity ratio of two species, a, the analyte and b, the internal standard molecularly dispersed within a single solution is given by Eq. 5:

$$\frac{I^a_m(\nu_0)}{I^b_m(\nu_0)} = \frac{N_aI_0F(n,\theta)S(\nu_0 - \upsilon)E(\nu_0 - \upsilon)\sigma^a_m(\nu_0)}{N_bI_0F(n',\theta)S(\nu_0 - \upsilon')E(\nu_0 - \upsilon')\sigma^b_m(\nu_0)} \sim \frac{N_a \cdot \sigma^a_m(\nu_0)}{N_b \cdot \sigma^b_m(\nu_0)} \tag{5}$$

$$\sigma^a_m(\nu_0) \sim \frac{I^a_m(\nu_0)}{I^b_m(\nu_0)} \cdot \frac{N_b}{N_a} \cdot \sigma^b_m(\nu_0) \tag{6}$$

Equation 6 shows that the common internal standard method of determining the analyte Raman cross-section $[\sigma^a_m(\nu_0)]$ from the ratio of observed intensities of the analyte to that of the internal standard only requires knowing the relative concentrations of the analyte (N_a) and internal standard molecules (N_b), as well as the internal standard Raman cross-section $[\sigma^b_m(\nu_0)]$, assuming negligible differences between $F(n, \theta)$ and $F(n', \theta)$, $S(\nu_0 - \upsilon)$ and $S(\nu_0 - \upsilon')$, and $E(\nu_0 - \upsilon)$ and $E(\nu_0 - \upsilon')$ at the Raman scattered frequency of the analyte $(\nu_0 - \upsilon)$ versus that at the internal standard $(\nu_0 - \upsilon')$, respectively. The subscript m indicates the sample solution.

The local field effect causes the Raman cross-sections of molecules with identical Raman polarizabilities to show different Raman cross-sections, and, thus, scatter with different Raman intensities in media of different refractive index. Equation 3 indicates that the local field correction increases the Raman cross-section in the pure liquid if its refractive index exceeds that of the solution sample. The solution Raman cross-sections of the analyte and internal standard can be related to their pure molecule Raman cross-sections by Eq. 3.

We can calculate the analyte pure liquid Raman cross-section from that measured in the solution with the dissolved internal standard if we know the pure internal standard Raman cross-section. Substituting the $\sigma^a_m(\nu_0)$ and $\sigma^b_m(\nu_0)$ in Eq. 6 with that of the pure analyte $[\sigma^a_\ell(\nu_0)]$ and pure internal standard Raman cross-sections $[\sigma^b_\ell(\nu_0)]$ and including the local field correction, we can write the relationship between the pure analyte Raman cross-section to that of pure internal standard (Eq. 7, the subscript ℓ indicates pure liquid or solid compound state). Therefore, the pure liquid analyte Raman cross-section $[\sigma^a_\ell(\nu_0)]$ can be calculated from the observed Raman intensity ratio $[I^a_m(\nu_0)/I^b_m(\nu_0)]$, the concentration ratio (N_b/N_a), the refractive indices $(n^a_\ell, n_m, n^b_\ell)$, and the pure internal standard Raman cross-section $\sigma^b_\ell(\nu_0)$

$$\sigma^a_\ell(\nu_0) = \frac{I^a_m(\nu_0)}{I^b_m(\nu_0)} \cdot \frac{N_b}{N_a} \cdot \left[\frac{(n^a_\ell/n_m)^2 + 2}{(n^b_\ell/n_m)^2 + 2}\right]^4 \sigma^b_\ell(\nu_0) \tag{7}$$

Chloroform 244 nm UV Raman Cross-section Determination. Figure 3 shows the UV Raman spectra of pure acetonitrile, pure chloroform, and a chloroform/acetonitrile mixture (volume ratio, 1 : 3). The 668 and 918 cm^{-1} bands

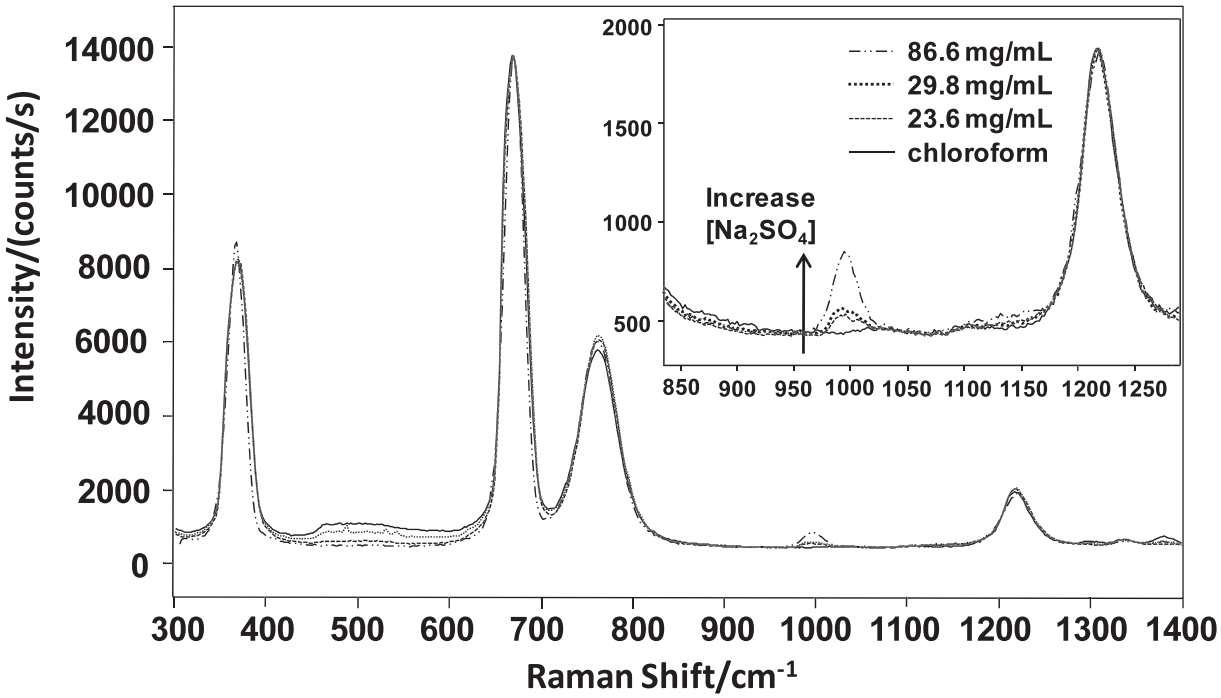

FIG. 4. UV Raman spectra of liquid chloroform and chloroform with increasing amounts of solid Na_2SO_4 particles of 23.6 mg/mL, 29.8 mg/mL, and 86.6 mg/mL. Raman spectra were normalized to the chloroform 668 cm^{-1} band.

derive from the liquid chloroform ν3 symmetric stretching mode[32] and the liquid acetonitrile ν4 C–C stretching mode,[33] respectively. The measured relative Raman intensity [$I_m^a(668)/I_m^b(918) = 1.86$] was obtained by integrating the Fig. 3 Raman bands of the $CHCl_3/CH_3CN$ solution (solid line). The aqueous solution 918 cm^{-1} acetonitrile (3.8 M) Raman cross-section was been reported by Asher et al. as 2.66×10^{-29} cm^2/(molc·sr) at 244 nm excitation.[10] Given a calculated 1.382 refractive index of this acetonitrile aqueous solution, close to that of pure acetonitrile, we calculate a similar Raman cross-section to that of the pure liquid acetonitrile [$\sigma_\ell^b(918)$] of 2.70×10^{-29} cm^2/(molc·sr) using Eq. 3.

The relative concentration of the chloroform and acetonitrile [$N_a(668)/N_b(918) = 0.215$] was calculated from the volume ratio (1 : 3) and densities (1.474 g/mL for chloroform, 0.787 g/mL for acetonitrile). The refractive indices of chloroform and acetonitrile are 1.53 and 1.39 at 244 nm, respectively.[24,34] We calculated a solution refractive index of 1.425 at 244 nm. By using Eq. 7, we calculate a pure liquid chloroform 244 nm UV Raman cross-section for the 668 cm^{-1} band of $\sigma_\ell^a(668) = 3.00 \pm 0.09 \times 10^{-28}$ cm^2/(molc·sr).

244 nm UV Raman Spectra of Chloroform and Na_2SO_4/Chloroform. Figure 4 shows the 244 nm Raman spectra for the Na_2SO_4/chloroform dispersions of Na_2SO_4 particles. We calculated Na_2SO_4 concentrations of 23.6 mg/mL (mole ratio 1 : 73.7), 29.8 mg/mL (mole ratio 1 : 58.1), and 86.6 mg/mL (mole ratio 1 : 19.6), respectively. The measured relative intensities of the 995 cm^{-1} SO_4^{2-} symmetric stretching band to that of the liquid chloroform 668 cm^{-1} band [$I_m^a(995)/I_m^b(668)$], that were obtained by integrating the Raman bands in Fig. 4 increased from 0.0091, to 0.0108, and 0.0342 as the solid Na_2SO_4 concentration increased from 23.6 mg/mL, to 29.8 mg/mL, and 86.6 mg/mL, respectively.

Because of the very similar refractive index of chloroform to that of solid Na_2SO_4 at 244 nm, the local field correction factor should be close to 1.0 and will not impact the Raman cross-section. We calculate the solid 244 nm UV Raman cross-sections for the 995 cm^{-1} SO_4^{2-} symmetric stretch band of $2.01 \pm 0.08 \times 10^{-28}$, $1.88 \pm 0.07 \times 10^{-28}$, and $2.01 \pm 0.07 \times 10^{-28}$ cm^2/(molc·sr) for these three different sample concentrations, respectively, giving an average solid 244 nm UV Raman cross-section for the 995 cm^{-1} SO_4^{2-} band of $1.97 \pm 0.07 \times 10^{-28}$ cm^2/(molc·sr). This value is around half of the aqueous Raman cross-section of 3.54×10^{-28} cm^2/(molc·sr) at 244 nm. The difference is close to the solid and solution $NaNO_3$ Raman cross-section difference reported by Asher et al.,[23] which is dominated by chemical differences between the solid state and solution state.[23]

By using the wavelength dispersion relationship for the solution 981 cm^{-1} SO_4^{2-} band, we can calculate that the 229 nm solid Raman cross-section for the 995 cm^{-1} SO_4^{2-} band is 2.74×10^{-28} cm^2/(molc·sr) compared to an aqueous solution value of 4.94×10^{-28} cm^2/(molc·sr) at 229 nm excitation.[10]

UV Raman Spectra of Acetonitrile and Na_2SO_4/Acetonitrile. For comparison, we also measured the solid sulfate Raman intensities in a liquid that was not refractive-index matched to the solid particles. Figure 5 shows the 244 nm UV Raman spectra of solid Na_2SO_4 dispersed in pure acetonitrile containing Na_2SO_4 particles at concentrations of 19.4 mg/mL (mole ratio 1 : 136.6), 29.0 mg/mL (mole ratio 1 : 90.6), and 52.1 mg/mL (mole ratio 1 : 48.8). Figure 5 also shows the neat acetonitrile spectrum. The increasing stray light background observed between 400 and 800 cm^{-1} indicates that elastic scattering is increased as the solid sulfate concentration increases in this non-refractive-index-matched solution. As the Na_2SO_4 particle concentration increases, the integrated relative Raman intensity ratio $I_m^a(995)/I_m^b(918)$ increases from 0.0347, to 0.0572, to 0.118.

Unlike the dissolved solution, for the Na_2SO_4 particle/acetonitrile dispersion both the acetonitrile and solid Na_2SO_4

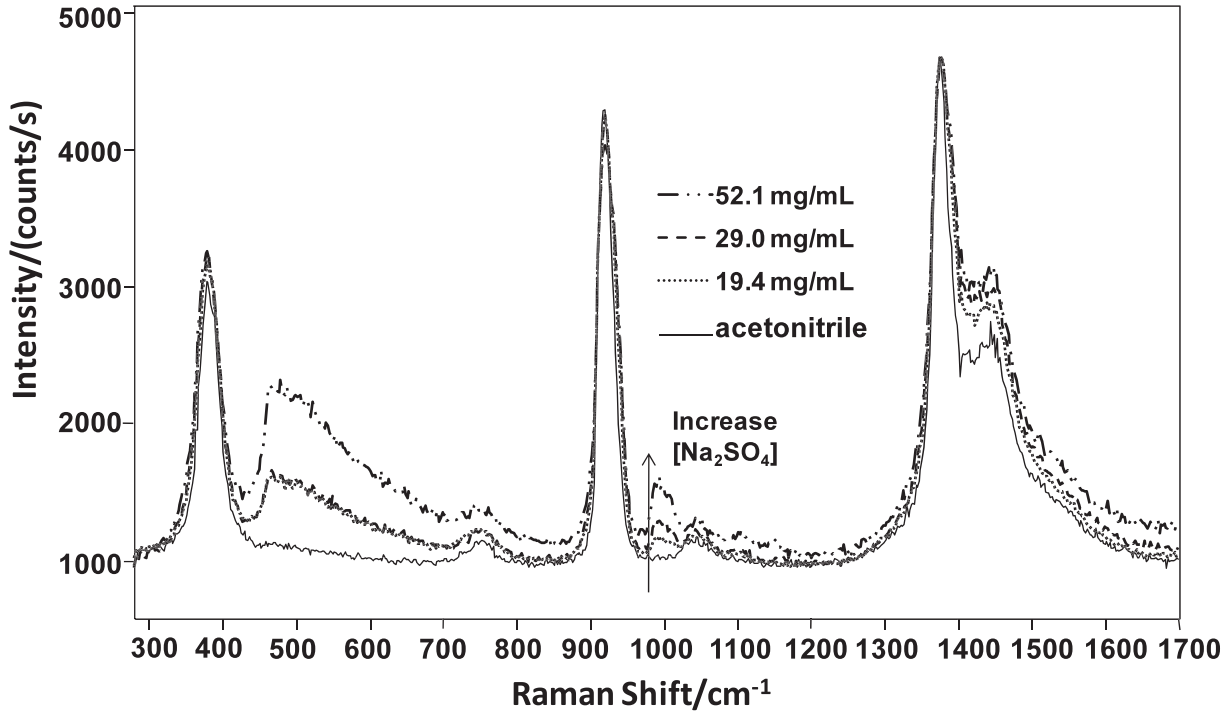

FIG. 5. UV Raman spectra of liquid acetonitrile and acetonitrile with increasing amounts of solid Na_2SO_4 particles of 19.4 mg/mL, 29.0 mg/mL, and 52.1 mg/mL. Raman spectra were normalized to the acetonitrile 1375 cm^{-1} band.

molecules are in their own pure phases with their particular refractive indices. Therefore, Eq. 7 becomes independent of the refractive indices, and we calculate solid-state 995 cm^{-1} SO_4^{2-} band 244 nm Raman cross-sections of $1.28 \pm 0.04 \times 10^{-28}$, $1.40 \pm 0.04 \times 10^{-28}$, and $1.55 \pm 0.05 \times 10^{-28}$ $cm^2/(molc \cdot sr)$ as the Na_2SO_4 particle concentration increases. The average solid 244 nm UV Raman cross-sections for the 995 cm^{-1} SO_4^{2-} band is $1.41 \pm 0.14 \times 10^{-28}$ $cm^2/(molc \cdot sr)$. This value is about 30% smaller than that found for solid Na_2SO_4 in chloroform. This decrease results from less penetration of the exciting light into the Na_2SO_4 particles because of the interface scattering of the incident light due to the refractive index difference between solid Na_2SO_4 and the acetonitrile.

We conclude that the refractive-index matching method used here is a fast and convenient method to determine solid particle Raman cross-sections because it avoids both the local field correction and interface scattering. In cases where a single solvent doesn't match the solid analyte's refractive index, one could use mixed solvents to match the refractive index and use the local field correction method.

CONCLUSIONS

We demonstrated a refractive-index matching method for determining the solid-state Na_2SO_4 particle 244 nm UV Raman cross-section. The 244 nm UV Raman cross-section of liquid chloroform was measured by using acetonitrile as an internal standard. The 244 nm Raman cross-section of liquid chloroform was found to be $3.00 \pm 0.09 \times 10^{-28}$ $cm^2/(molc \cdot sr)$. We then used liquid chloroform as an internal standard to determine that the solid Na_2SO_4 244 nm UV Raman cross-section of the 995 cm^{-1} symmetric stretching band is $1.97 \pm 0.07 \times 10^{-28}$ $cm^2/(molc \cdot sr)$. This is the first report of a method to measure nonabsorbing solid UV Raman cross-sections that avoids interface-scattering bias.

We also measured a 30% smaller value for the solid 995 cm^{-1} Na_2SO_4 Raman cross-sections when we attempted to use non-refractive-index matched acetonitrile. This 30% decrease results from the Na_2SO_4 particle interface scattering.

The refractive-index matching method provides a simple and accurate way to determine the solid-state particle Raman cross-sections, avoiding the use of the local field corrections and avoiding interface scattering bias. This method is useful for accurate determination of solid-state Raman cross-sections.

ACKNOWLEDGMENTS

We appreciate partial funding of this work by the West Virginia High Technology Consortium Foundation under contract number HSHQDC-09-C-00159 from the Department of Homeland Security Science and Technology Directorate. We also thank Hong Zhang from Dr. Weber's group at University of Pittsburgh for the help on the optical imaging of ground solid Na_2SO_4 particles.

1. I. R. Lewis and H. G. M. Edwards, *Handbook of Raman Spectroscopy: From the Research Laboratory to the Process Line* (Marcel Dekker, New York, 2001), p. 1.
2. S. A. Asher, Anal. Chem. **65,** 59A (1993).
3. S. A. Asher, Anal. Chem. **65,** 201A (1993).
4. C. M. Penney, L. M. Goldman, and M. Lapp, Nat. Phys. Sci. **235,** 110 (1972).
5. Y. Kato and H. Takuma, J. Opt. Soc. Am. **61,** 347 (1971).
6. L. J. Hughes, L. E. Steenhoek, and E. S. Yeung, Chem. Phys. Lett. **58,** 413 (1978).
7. K. T. Schomacker, J. K. Delaney, and P. M. Champion, J. Chem. Phys. **85,** 4240 (1986).
8. M. O. Trulson and R. A. Mathies, J. Chem. Phys. **84,** 2068 (1986).
9. B. E. Kincaid and J. R. Fontana, Appl. Phys. Lett. **28,** 12 (1976).
10. J. M. Dudik, C. R. Johnson, and S. A. Asher, J. Chem. Phys. **82,** 1732 (1985).
11. S. A. Asher and C. R. Johnson, J. Phys. Chem. **89,** 1375 (1985).

12. S. A. Asher, M. Ludwig, and C. R. Johnson, J. Am. Chem. Soc. **108,** 3186 (1986).
13. S. A. Asher and J. L. Murtaugh, Appl. Spectrosc. **42,** 83 (1988).
14. J. D. Lorentzen, S. Guha, j. Menéndez, P. Giannozzi, and S. Baroni, Chem. Phys. Lett. **270,** 129 (1997).
15. Z. Chi and S. A. Asher, J. Phys. Chem. B **102,** 9595 (1998).
16. Y. Tian, J. Zuo, L. Zhang, Z. Li, S. Gao, and G. Lu, Appl. Phys. B **87,** 727 (2007).
17. S. Shim, C. M. Stuart, and R. A. Mathies, ChemPhysChem **9,** 697 (2008).
18. M. J. Colles and J. E. Griffiths, J. Chem. Phys. **56,** 3384 (1972).
19. N. Abe, M. Wakayama, and M. Ito, J. Raman Spectrosc. **6,** 38 (1977).
20. E. D. Emmons, A. W. Fountain III, J. A. Guicheteau, and S. D. Christesen, XXII International Conference on Raman Spectroscopy AIP Conference Proceedings **1267,** 508 (2010).
21. E. D. Emmons, J. A. Guicheteau, A. W. Fountain III, and S. D. Christesen, "Comparison of Absolute Raman Cross Sections of Explosives in Solution and in the Solid State," Appl. Spectrosc., paper in preparation (2011).
22. L. Nagli, M. Gaft, Y. Fleger, and M. Rosenbluh, Opt. Mater. **30,** 1747 (2008).
23. L. Wang, D. Tuschel, and S. A. Asher, J. Phys. Chem. C **115,** 15767 (2011).
24. A. Samoc, J. Appl. Phys. **94,** 6167 (2003).
25. B. W. Smith, Y. Fan, M. Slocum, and L. Zavyalova, *Optical Microlithography XVIII*, B. W. Smith, Ed., Proceedings of the SPIE **5754,** 141 (2005).
26. S. A. Asher, R. W. Bormett, X. G. Chen, D. H. Lemmon, N. Cho, P. Peterson, M. Arrigoni, L. Spinelli, and J. Cannon, Appl. Spectrosc. **47,** 628 (1993).
27. D. D. Tuschel, A. V. Mikhonin, B. E. Lemoff, and S. A. Asher, Appl. Spectrosc. **64,** 425 (2010).
28. J. R. Nestor and E. R. Lippincott, J. Raman Spectrosc. **1,** 305 (1973).
29. G. Eckhardt and W. G. Wagner, J. Mol. Spectrosc. **19,** 407 (1966).
30. P. Mirone, Spectrochimica Acta **22,** 1897 (1966).
31. G. Fini, P. Mirone, and P. Patella, J. Mol. Spectrosc. **28,** 144 (1968).
32. M. V. Rao, Proc. Math. Sci. **24,** 510 (1946).
33. A. Loewenschuss and N. Yellin, Spectrochim. Acta, Part A **31,** 207 (1975).
34. J. R. Krivacic and D. W. Urry, Anal. Chem. **42,** 596 (1970).